Phase structure of difermion condensates in the Nambu–Jona-Lasinio model: The size-dependent properties

A Letters Journal Exploring the Frontiers of Physics

April 2010

EPL, **90** (2010) 11001
doi: 10.1209/0295-5075/90/11001

www.epljournal.org

Phase structure of difermion condensates in the Nambu–Jona-Lasinio model: The size-dependent properties

L. M. Abreu[1(a)], A. P. C. Malbouisson[2] and J. M. C. Malbouisson[1]

[1] *Instituto de Física, Universidade Federal da Bahia - 40210-340, Salvador, BA, Brazil*
[2] *Centro Brasileiro de Pesquisas Físicas, MCT - 22290-180, Rio de Janeiro, RJ, Brazil*

received 29 January 2010; accepted in final form 30 March 2010
published online 5 May 2010

PACS 11.10.Kk – Field theories in dimensions other than four
PACS 11.30.Qc – Spontaneous and radiative symmetry breaking
PACS 11.10.Wx – Finite-temperature field theory

Abstract – We investigate finite-size effects on the phase structure of difermion condensates at finite temperature and density in the framework of the two-dimensional large-N limit Nambu–Jona-Lasinio model. We take into account size-dependent effects on the system by making use of *zeta*-function and compactification methods. The thermodynamic potential and the gap equation for the difermion condensed phase are then derived in the mean-field approximation. Size-dependent critical lines separating trivial and non-trivial difermion condensed phases are obtained imposing either periodic or anti-periodic boundary conditions on the spatial coordinate.

Introduction. – The analysis of the phase diagram of strongly interacting matter has been a subject of great interest in recent years. Due to the complex field-theoretical structure of quantum chromodynamics (QCD), simplified effective theories, particularly in their low-dimensional versions, have been largely employed to get, analytically, insights on this phase structure. In this sense, four-fermion models, like the Nambu–Jona-Lasinio (NJL) model [1], are very useful for the investigation of the breakdown of dynamical symmetries. Nowadays the NJL model reveals convenient in the description of the phase diagram of both chiral broken phase (quark-antiquark condensation) and color superconducting phase (diquark condensation), specially with the system under certain conditions, like finite temperature, finite chemical potential, external gauge field, among others [2–4].

Another interesting aspect in the study of these kind of phase transitions is the relevance of the fluctuations due to finite-size effects in the phase diagram. With this purpose, different approaches have been used to study various aspects of these effects [5–17]. In this letter, we are interested in the investigation of the size dependence of the phase structure of difermion condensates, in the framework of the two-dimensional large-N NJL model at finite temperature and density. To include finite-size effects, we make use of the techniques introduced in refs. [16,17]. This is carried out through *zeta*-function regularization and compactification methods [18,19]. This approach allows to determine analytically the size-dependence of the effective potential and the gap equation. Then, phase diagrams at finite temperature and chemical potential, where the symmetric and difermion condensed phases are separated by size-dependent critical lines, are obtained.

Let us remark that our interest in the two-dimensional version of NJL model is an attempt to investigate the qualitative aspects relevant to the difermion condensation under the influence of size finiteness of the system. In fact some properties of these kind of models are similar in lower and higher dimensions, and so, we can expect that results obtained in the 2D NJL model reflect properties of a more realistic 4D model.

It could be argued that spontaneous symmetry breaking (SSB) does not occur in two-dimensional theories, as a consequence of the Mermin-Wagner-Coleman theorem [20]. The reason is that the presence of strong infrared fluctuations destroys the long-range order, and consequently the SSB is denied. However, as demonstrated in ref. [21], this theorem can be circumvented in the following way: in a N-component formulation, the two-point correlation function for a certain order parameter ϕ has the form $\langle\phi^*(x)\phi(y)\rangle \sim |x-y|^{-1/N}$. At finite N there is no

(a) E-mail: luciano.abreu@ufba.br

SSB in long range, as expected from the Mermin-Wagner-Coleman theorem. On the other hand, in the large-N limit, for $|x-y|\to\infty$ the two-point function becomes a non-vanishing constant, allowing the SSB. Thus, it is legitimate to study SSB effects in terms of low-dimensional NJL model in the large-N limit, as can be seen in the literature [5,6,15,22–30].

We organize the letter as follows. We start by calculating the effective potential of the NJL model in the mean-field approximation, using the *zeta*-function method. The analysis of symmetry breaking induced by the difermion condensate is also done. In the following, the size-dependent gap equation is discussed. After, the phase diagrams are shown and analyzed. We finalize presenting some concluding remarks.

The model. – Our starting point is the two-dimensional massless version of the extended NJL model described by the Lagrangian density [23,24,27],

$$\begin{aligned}\mathcal{L} \,=\, & \bar{\psi}^{(i)}\,\left(i\,\partial\!\!\!/-\mu\gamma^0\right)\,\psi^{(i)}+\frac{g_S}{2}\left(\bar{\psi}^{(i)}\psi^{(i)}\right)^2\\ & +g_D\left(\bar{\psi}^{(i)}\gamma_5\psi^{(j)}\right)\left(\bar{\psi}^{(i)}\gamma_5\psi^{(j)}\right),\end{aligned}\tag{1}$$

where ψ and $\bar{\psi}$ are the fermion fields carrying N flavors ($i,j=1,\ldots,N$; repeated flavor indices are summed), μ is the chemical potential and the γ matrices are in a representation of two-dimensional space, with $\gamma^5=\gamma^0\gamma^1$. Notice that the Lagrangian density possess $O(N)$ flavor symmetry and discrete chiral symmetry.

We choose the particular representation for the γ-matrices

$$\gamma^0=\begin{pmatrix}0 & 1\\ 1 & 0\end{pmatrix},\qquad \gamma^1=\begin{pmatrix}0 & -1\\ 1 & 0\end{pmatrix}.\tag{2}$$

In this case, the charge conjugation is implemented by $C=-\gamma^1$. Then, the pairing term reads

$$\begin{aligned}& g_D\left(\bar{\psi}^{(i)}\gamma_5\psi^{(j)}\right)\left(\bar{\psi}^{(i)}\gamma_5\psi^{(j)}\right)=\\ & -\frac{g_D}{2}\left(\varepsilon_{\alpha\beta}\psi^{\dagger(i)}_{\alpha}\psi^{\dagger(i)}_{\beta}\right)\left(\varepsilon_{\gamma\delta}\psi^{(j)}_{\gamma}\psi^{(j)}_{\delta}\right).\end{aligned}\tag{3}$$

Since we are specifically interested on size effects of the pure difermion condensate sector, to make the treatment clearer, we suppress the scalar self-interaction setting $g_S=0$ in the Lagrangian density (1).

We perform the bosonization by introducing the auxiliary field Δ such that it is associated with the bilinear form in the way: $g_D\varepsilon_{\gamma\delta}\psi^{(j)}_{\gamma}\psi^{(j)}_{\delta}\equiv\Delta$. Therefore the modified Lagrangian density becomes

$$\begin{aligned}\widetilde{\mathcal{L}} \,=\, & \bar{\psi}^{(i)}\,\left(i\,\partial\!\!\!/-\mu\gamma^0\right)\,\psi^{(i)}-\frac{1}{2}\Delta^{\dagger}\left(\varepsilon_{\gamma\delta}\psi^{(j)}_{\gamma}\psi^{(j)}_{\delta}\right)\\ & +\frac{1}{2}\left(\varepsilon_{\alpha\beta}\psi^{\dagger(i)}_{\alpha}\psi^{\dagger(i)}_{\beta}\right)\Delta-\frac{1}{2g_D}|\Delta|^2.\end{aligned}\tag{4}$$

Thus, the auxiliary field Δ plays the role of a difermion condensate, such that when it has a non-vanishing value, the system is in difermion condensation phase.

Then integration over ψ and $\psi^{\dagger}$ generates the following effective action:

$$\Gamma_{eff}(|\Delta|)\,=\,\int \mathrm{d}^2x\left(-\frac{1}{2g_D}|\Delta|^2\right)-\frac{i}{2}\mathrm{Tr}\ln D,\tag{5}$$

where

$$D=\begin{pmatrix}-h & \gamma^1\Delta^{\dagger}\\ -\gamma^1\Delta & h^T\end{pmatrix},\tag{6}$$

with

$$\begin{aligned}h \,&=\, i\partial_0+i\gamma^5\partial_1-\mu,\\ h^T&=-i\partial_0-i\gamma^5\partial_1-\mu.\end{aligned}\tag{7}$$

Notice that the trace over the flavor indices in eq. (5) gives a factor N, which allow us to set in the large-N limit $g_DN=G_D$, with G_D fixed at $N\to\infty$. Thus, the effective potential is obtained in the mean-field approximation (*i.e.* $|\Delta|$ uniform) from eq. (5),

$$\begin{aligned}U_{eff}(\Delta) \,=\, & \frac{|\Delta|^2}{2G_D}+\frac{i}{2}\mathrm{tr}\ln\left(h^Th\right)\\ & +\frac{i}{2}\mathrm{tr}\ln\left[1-|\Delta|^2(h^T)^{-1}\gamma^1(h)^{-1}\gamma^1\right],\end{aligned}\tag{8}$$

where tr means trace over spins and coordinates only.

To take into account finite-temperature and finite-size effects on the phase structure of this model, we work in the Euclidean space, with imaginary time and the spatial coordinate being compactified. We denote the Euclidean coordinate vectors by $x_E=(x_0,x)$, in which $x_0\in[0,\beta]$ and $x\in[0,L]$, with $\beta=T^{-1}$ (T being the temperature and L is the size of the system). This corresponds to the generalized Matsubara prescription,

$$\begin{aligned}\int\frac{\mathrm{d}^2p}{(2\pi)^2}f(p_0,p) \,&\to\, \frac{1}{\beta L}\sum_{n_0,n=-\infty}^{\infty}f(p_{n_0},p_n),\\ p_0\,&\to\, p_{n_0}=\frac{2\pi}{\beta}\left(n_0+\frac{1}{2}\right);\quad n_0\in\mathbb{Z},\\ p\,&\to\, p_n=\frac{2\pi}{L}\left(n+c\right);\quad n\in\mathbb{Z},\end{aligned}$$

where $c=0$ and $c=\frac{1}{2}$ for periodic and for antiperiodic spatial boundary conditions, respectively.

Thus, after some manipulations, the effective potential carrying finite-temperature and finite-size effects becomes, by omitting terms independent of $|\Delta|$,

$$\begin{aligned}U^{\beta,L}_{eff}(|\Delta|) \,=\, & \frac{|\Delta|^2}{2G_D}\\ & -\frac{1}{2\beta L}\sum_{\pm}\sum_{n_0,n=-\infty}^{\infty}\ln\left[\frac{4\pi^2}{\beta^2}\left(n_0+\frac{1}{2}\right)^2\right.\\ & \left.+\frac{4\pi^2}{L^2}\left(|n+c|\pm\frac{\mu L}{2\pi}\right)^2+|\Delta|^2\right].\end{aligned}\tag{9}$$

The effective potential in eq. (9) can be rewritten in terms of Epstein *zeta*-functions, $Y(s)$, that is

$$U_{eff}^{\beta,L}(|\Delta|) = \frac{|\Delta|^2}{2G_D} + \frac{1}{2\beta L}\sum_{\pm}\frac{\mathrm{d}}{\mathrm{d}s}\,Y_{\Delta}^{\pm}(s)\big|_{s=0}, \quad (10)$$

where

$$Y_{\Delta}^{\pm}(s) = \sum_{n_0,n=-\infty}^{\infty}\left[\frac{4\pi^2}{\beta^2}\left(n_0+\frac{1}{2}\right)^2 + \frac{4\pi^2}{L^2}\left(|n+c|\pm\frac{\mu L}{2\pi}\right)^2 + |\Delta|^2\right]^{-s}. \quad (11)$$

Hence, the analysis of the phase diagram of the model is performed through the solutions of the gap equation

$$\frac{\partial}{\partial|\Delta|}U_{eff,R}^{\beta,L}(|\Delta|) = 0, \quad (12)$$

from which we find that Δ appears here as the order parameter of the difermion condensate phase transition.

So, in the following we discuss the size effects on the gap equation. However, for completeness and to set up the free space parameters, in the next section we treat the model in the absence of spatial boundaries at zero temperature.

The model at zero-temperature and without spatial boundaries. – Let us look at the model introduced in the previous section without compactification of the spatial dimension [31] and at zero temperature. Taking $\mu = T = 1/L = 0$ in eq. (8), the renormalization condition is

$$\frac{1}{G_{DR}} = \frac{\partial^2}{\partial|\Delta|^2}U_{eff}(|\Delta|)\Big|_{|\Delta|=\lambda} = \frac{1}{G_D} - \left[\frac{(D-1)}{(4\pi)D/2}\Gamma\left(1-\frac{D}{2}\right)\lambda^{D-2}\right]_{D=2}, \quad (13)$$

where λ is a scale parameter and G_{DR} is the renormalized coupling constant.

In this case the gap equation is

$$\frac{\partial}{\partial|\Delta|}U_{eff}(|\Delta|)\Big|_{|\Delta|=\Delta_0} = 0, \quad (14)$$

where Δ_0 is the order parameter for the model at zero temperature, in the absence of spatial boundaries and at vanishing chemical potential. Then, in terms of the renormalized coupling constant, we obtain

$$\frac{1}{G_{DR}} = \frac{1}{2\pi} - \frac{1}{4\pi}\ln\frac{\Delta_0^2}{\lambda^2}. \quad (15)$$

It results from eqs. (13)–(15), that we can write the renormalized effective potential as

$$U_{eff,R}(|\Delta|) = \frac{|\Delta|^2}{2}\left(-\frac{1}{4\pi} + \frac{1}{4\pi}\ln\frac{|\Delta|^2}{\Delta_0^2}\right). \quad (16)$$

Hence, at gap solution $|\Delta| = \Delta_0$, eq. (16) yields

$$U_{eff,R}(\Delta_0) = -\frac{\Delta_0^2}{8\pi}, \quad (17)$$

which is similar to that obtained in refs. [23,24].

The model at finite temperature and with the presence of spatial boundaries. – Now we can analyze the model taking into account temperature, chemical potential and finite-size effects. To proceed, the renormalization prescription performed in the previous section allows us to work with the T, μ, L-dependent renormalized effective potential, written as

$$U_{eff,R}^{\beta,L}(|\Delta|) = -\frac{1}{4\pi}|\Delta|^2\ln\frac{\Delta_0}{\lambda} + \frac{1}{2\beta L}\sum_{\pm}\mathrm{FP}\left[\frac{\mathrm{d}}{\mathrm{d}s}\,Y_{\Delta}^{\pm}(s)\big|_{s=0} + \ln\lambda^2 Y_{\Delta}^{\pm}(0)\right], \quad (18)$$

where FP[...] means the finite part of the terms between brackets; this notation is in agreement with refs. [16,18].

To study the solutions of the gap equation (12), we must perform the analytical continuation of the Epstein *zeta*-function $Y_{\Delta}^{\pm}$ in eq. (11), given by [16–18]

$$Y_{\Delta}^{\pm}(s) = \frac{\beta}{2\pi}\frac{\Gamma\left(s-\frac{1}{2}\right)}{\Gamma(s)}\left(\frac{4\pi^2}{L^2}\right)^{-s}\sum_{\pm}\left[\zeta\left(2\,s, c\pm\frac{\mu L}{2\pi}\right) + \zeta\left(2\,s, 1-c\mp\frac{\mu L}{2\pi}\right)\right] + \frac{2\beta}{2^{s-\frac{1}{2}}\sqrt{\pi}\Gamma(s)}\sum_{\pm}\sum_{n_0=1}^{\infty}\sum_{n=-\infty}^{\infty}(-1)^{n_0} \times\left(\frac{n_0\beta}{\sqrt{\frac{4\pi^2}{L^2}\left(|n+\frac{1}{2}|\pm\frac{\mu L}{2\pi}\right)^2+|\Delta|^2}}\right)^{s-\frac{1}{2}} \times K_{s-\frac{1}{2}}\left(n_0\beta\sqrt{\frac{4\pi^2}{L^2}\left(|n+\frac{1}{2}|\pm\frac{\mu L}{2\pi}\right)^2+|\Delta|^2}\right), \quad (19)$$

where $\zeta(s,a) = \sum_{n=0}^{\infty}(n+a)^{-s}$ is the Hurwitz *zeta*-function. Also, we have fixed λ as the scale of the model, redefining the relevant quantities as $\Delta_0/\lambda \to \Delta_0$, $L\lambda \to L$, $\mu/\lambda \to \mu$ and $\beta\lambda \to \beta$.

Notice that for the gap equation the Epstein *zeta*-function in eq. (19) is taken at $s = 1$. Thus, the gap equation (already without the infinities, suppressed

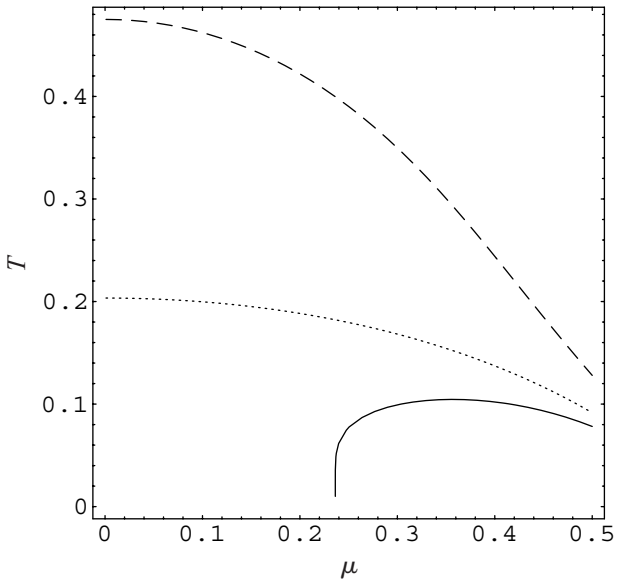

Fig. 1: The phase diagram in the (μ, T)-plane, at fixed $x = L^{-1} = 0.2$ in the antiperiodic case. Dashed, dotted and solid lines represent $\Delta_0 = 1, 1/4$ and $1/8$, respectively. The difermion condensate region corresponds to the region below each line.

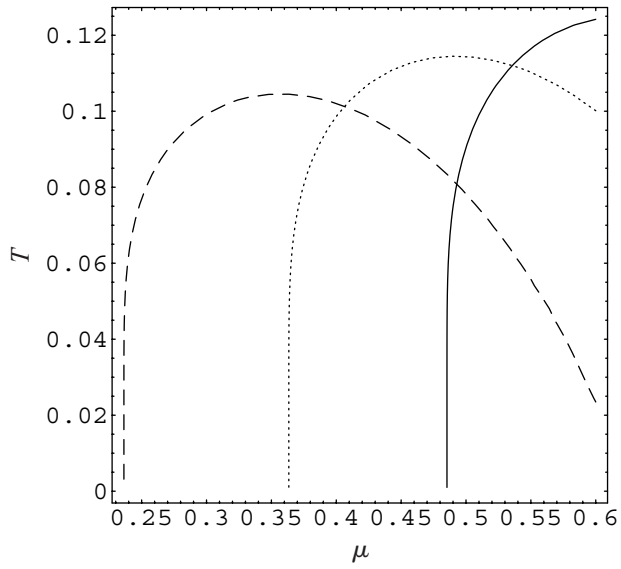

Fig. 2: The phase diagram in the (μ, T)-plane, at $\Delta_0 = 1/8$ in the antiperiodic case. Dashed, dotted and solid lines represent the values $x = L^{-1} = 0.2, 0.25$ and 0.3, respectively. The difermion condensate region corresponds to the region below each line.

by minimal subtraction) in the particular situation of $\Delta \to 0$ is

$$
\begin{aligned}
&-2\ln\frac{\Delta_0 L}{4\pi}+\psi\left(\frac{1}{2}+\frac{\mu L}{2\pi}\right)+\psi\left(\frac{1}{2}-\frac{\mu L}{2\pi}\right)\\
&-\frac{4}{L}\sum_{\pm}\sum_{n_0=1}^{\infty}\sum_{n=-\infty}^{\infty}(-1)^{n_0}\left(\frac{n_0\beta}{\sqrt{\frac{4\pi^2}{L^2}\left(|n+\frac{1}{2}|\pm\frac{\mu L}{2\pi}\right)^2}}\right)^{\frac{1}{2}}\\
&\times K_{\frac{1}{2}}\left(n_0\beta\sqrt{\frac{4\pi^2}{L^2}\left(|n+\frac{1}{2}|\pm\frac{\mu L}{2\pi}\right)^2}\right)=0, \qquad (20)
\end{aligned}
$$

for antiperiodic conditions on the spatial coordinate, and

$$
\begin{aligned}
&-2\ln\frac{\Delta_0 L}{4\pi}+\psi\left(\frac{\mu L}{2\pi}\right)+\psi\left(1+\frac{\mu L}{2\pi}\right)+2\psi\left(1-\frac{\mu L}{2\pi}\right)\\
&+\frac{2\pi}{\mu L}-\frac{4}{L}\sum_{\pm}\sum_{n_0=1}^{\infty}\sum_{n=-\infty}^{\infty}(-1)^{n_0}\\
&\times\left(\frac{n_0\beta}{\sqrt{\frac{4\pi^2}{L^2}\left(|n|\pm\frac{\mu L}{2\pi}\right)^2}}\right)^{\frac{1}{2}}\\
&\times K_{\frac{1}{2}}\left(n_0\beta\sqrt{\frac{4\pi^2}{L^2}\left(|n|\pm\frac{\mu L}{2\pi}\right)^2}\right)=0, \qquad (21)
\end{aligned}
$$

for periodic conditions.

Phase structure. – Now let us analyze the size-dependent fermion-fermion pairing phase structure. We remark that the gap equations (20) and (21) in the previous section were obtained in the limit $\Delta \to 0$, which is appropriate for a second-order phase transition between the symmetric phase and the difermion condensed phase.

In fig. 1 the phase diagram in the (T, μ)-plane is displayed in the cases of different values of Δ_0 at a fixed value of $x = 1/L$ for the gap equation in eq. (20) (antiperiodic boundary conditions). In accordance with the results of ref. [31] for the system in bulk form, for small values of Δ_0 the difermion condensed phase appears at low temperature and at high chemical potential; this is expected in phase diagrams of strongly interacting matter. On the other hand, as Δ_0 increases, the difermion condensed phase region enlarges, reaching low values of μ and higher values of T.

In fig. 2 is plotted the phase diagram of the system in the (T, μ)-plane at fixed Δ_0, but with different values of the inverse of the size of the system, $x = 1/L$, in the antiperiodic case. The values of the chemical potential for which the system undergoes the phase transition are $\mu \approx 0.24, 0.36$ and 0.48 for $x = L^{-1} = 0.2, 0.25$ and 0.3, respectively, for the choice $\Delta_0 = 1/8$. Thus, we see that when the size of the system decreases, greater values of the chemical potential are necessary to reach the difermion condensed phase region. On the other hand, for smaller sizes, this region can be reached for greater temperatures.

The case of periodic boundary conditions corresponds to the gap equation given by eq. (21). The phase structure in the (T, μ)-plane is displayed in figs. 3 and 4. In fig. 3 different values of Δ_0 are taken at fixed $x = 1/L$, while in fig. 4 different values of $x = 1/L$ at fixed Δ_0 are considered. The properties of these phase diagrams are

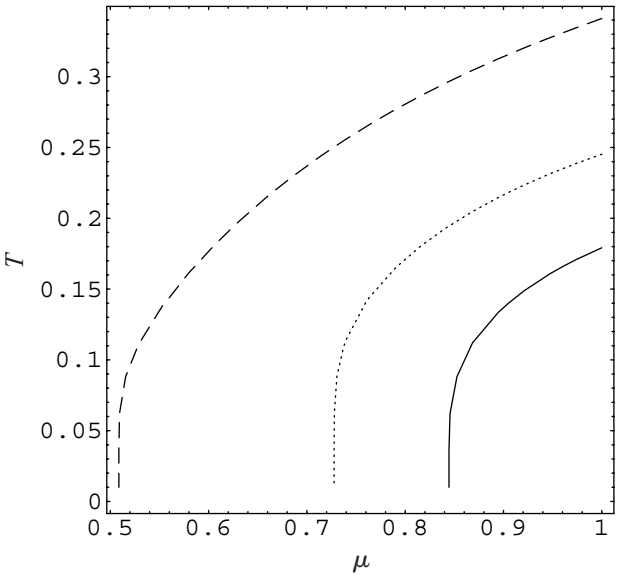

Fig. 3: The phase diagram in the (μ, T)-plane, at fixed $x = L^{-1} = 0.2$ in the periodic case. Dashed, dotted and solid lines represent $\Delta_0 = 1/4, 1/8$ and $1/16$, respectively. The difermion condensate region corresponds to the region below each line.

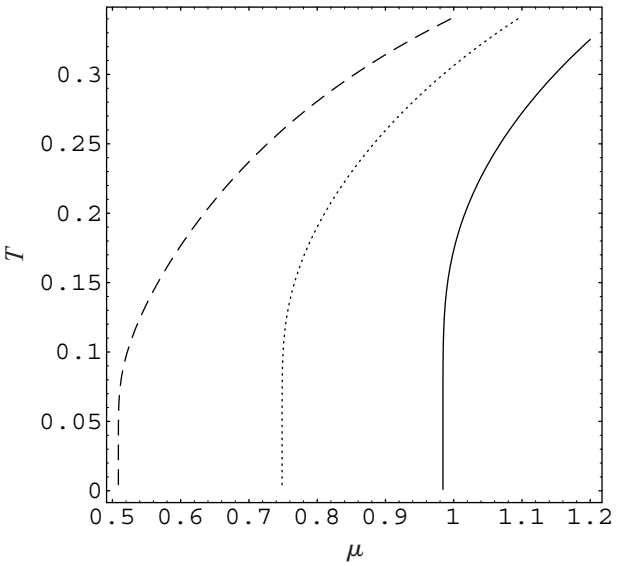

Fig. 4: The phase diagram in the (μ, T)-plane, at $\Delta_0 = 1/4$ in the periodic case. Dashed, dotted and solid lines represent the values $x = L^{-1} = 0.2, 0.25$ and 0.3, respectively. The difermion condensate region corresponds to the region below each line.

similar to those in the antiperiodic case. The difference is in the choice of values of Δ_0 giving similar results. This can be seen comparing figs. 1 and 3, and also in the comparison between figs. 2 and 4. The periodic situation fits qualitatively better with the phase diagram of strongly interacting matter for greater values of Δ_0 than in the antiperiodic case. In addition, from fig. 4, we observe that the phase transition occurs at $\mu \approx 0.51, 0.75$ and 0.98 for $x = L^{-1} = 0.2, 0.25$ and 0.3, respectively, for the choice $\Delta_0 = 1/4$.

Concluding remarks. – In this work we have investigated finite-size effects on the phase structure of difermion condensates at finite temperature and density, in the framework of the two-dimensional NJL model in the large-N limit. We have employed *zeta*-function regularization and compactification methods in the mean-field approximation.

The phase structure of this model was studied from the gap equation. Then, size-dependent critical curves that separate the symmetric and the difermion condensed phases for a second-order phase transition have been obtained for antiperiodic and periodic boundary conditions on the spatial coordinate.

We have seen that the critical lines are sensitive to changes of the parameter Δ_0; in particular, the case of antiperiodic boundary conditions needs lower values of Δ_0 to generate, with respect to the periodic case, a phase diagram qualitatively similar to the one expected for strongly interacting matter.

In addition, we have shown that, as the size of the system decreases, greater values of the chemical potential are necessary to reach the region of difermion condensed phase, in both situations of antiperiodic and periodic boundary conditions. Possible extensions of this work are the investigation of the model in four dimensions, as well as the study of full phase structure.

* * *

This work received partial financial support from CNPq (Brazilian National Research Council).

REFERENCES

[1] Nambu Y. and Jona-Lasinio G., *Phys. Rev.*, **122** (1961) 345; **124** (1961) 246.
[2] Klevansky S. P., *Rev. Mod. Phys.*, **27** (1991) 195.
[3] Hatsuda T. and Kunihiro T., *Phys. Rep.*, **247** (1994) 221.
[4] Buballa M., *Phys. Rep.*, **407** (2005) 205.
[5] Song D. Y. and Kim J. K., *Phys. Rev. D*, **41** (1990) 3165.
[6] Song D. Y., *Phys. Rev. D*, **46** (1992) 737.
[7] Kim D. K., Han Y. D. and Koh I. G., *Phys. Rev. D*, **49** (1994) 6943.
[8] He Y. B., Chao W. Q., Gao C. S. and Li X. Q., *Phys. Rev. C*, **54** (1996) 857.
[9] Vshivtsev A. S., Vdovichenko M. A. and Klimenko K. G., *J. Exp. Theor. Phys.*, **87** (1998) 229.
[10] Kogut J. B. and Strouthos C. G., *Phys. Rev. D*, **63** (2001) 054502.
[11] Kiriyama O. and Hosaka A., *Phys. Rev. D*, **67** (2003) 085010.
[12] Beneventano C. G. and Santangelo E. M., *J. Phys. A*, **37** (2004) 9261.

[13] Gamayun A. V. and Gorbar E. V., *Phys. Lett. B*, **610** (2005) 74.
[14] Kiriyama O., Kodama T. and Koide T., hep-ph/0602086, preprint (2006); Palhares L. F., Fraga E. S. and Kodama T., hep-ph/0910.4363v1, preprint (2009); hep-ph/0904.4830, preprint (2009).
[15] Ebert D., Klimenko K. G., Tyukov A. V. and Zhukovsky V. C., *Phys. Rev. D*, **78** (2008) 045008; *Eur. Phys. J. C*, **58** (2008) 57.
[16] Abreu L. M., Gomes M. and da Silva A. J., *Phys. Lett. B*, **642** (2006) 551.
[17] Abreu L. M., Malbouisson A. P. C., Malbouisson J. M. C. and Santana A. E., *Nucl. Phys. B*, **819** (2009) 127.
[18] Elizalde E., *Ten Physical Applications of Spectral Zeta Function, Lect. Notes Phys.* (Springer-Verlag, Berlin) 1995.
[19] Malbouisson A. P. C., Malbouisson J. M. C. and Santana A. E., *Nucl. Phys. B*, **631** (2002) 83.
[20] Mermin N. D. and Wagner H., *Phys. Rev. Lett.*, **17** (1966) 1133; Coleman S., *Commun. Math. Phys.*, **31** (1973) 259.
[21] Witten E., *Nucl. Phys. B*, **145** (1978) 110.
[22] Barducci A., Casalbuoni R., Modugno M., Pettini G. and Gatto R., *Phys. Rev. D*, **51** (1995) 3042.
[23] Chodos A., Minakata H. and Cooper F., *Phys. Lett. B*, **449** (1999) 260.
[24] Chodos A., Cooper F., Mao W., Minakata H. and Singh A., *Phys. Rev. D*, **61** (2000) 045011.
[25] Schoen V. and Thies M., hep-th/0008175, preprint (2000); Brzoska A. and Thies M., *Phys. Rev. D*, **65** (2002) 125001.
[26] Ohwa K., *Phys. Rev. D*, **65** (2002) 085040.
[27] Mihaila B., Blagoev K. and Cooper F., *Phys. Rev. D*, **73** (2006) 016005.
[28] Kneur J. L., Pinto M. B. and Ramos R. O., *Phys. Rev. D*, **74** (2006) 125020; *Int. J. Mod. Phys. E*, **16** (2007) 2798.
[29] Basar G., Dunne G. V. and Thies M., *Phys. Rev. D*, **79** (2009) 105012.
[30] Zhou B. R., *Commun. Theor. Phys.*, **47** (2007) 520; hep-th/0703060v1, preprint (2007).
[31] Kohyama H., *Phys. Rev. D*, **77** (2008) 045016; hep-th/0805.0003, preprint (2008).